BNL-21794

A MODEL FOR RAIN COMPOSITION AND THE WASHOUT OF SULFUR DIOXIDE*

by

F.B. Hill and R.F. Adamowicz
Department of Applied Science
Brookhaven National Laboratory
Upton, New York 11973

July 1976

Prepared for presentation in AIChE 69th Annual Meeting, Chicago, Illinois, November 28-December 2, 1976.

*Work carried out under the auspices of the U.S. Energy Research and Development Administration.

DISCLAIMER

ABSTRACT

A continuous model for the washout of sulfur dioxide from the atmosphere by rain was developed in which account was taken of mass transfer of SO_2 into well-mixed drops, ionic equilibrium of sulfur compounds in solution, oxidation of dissolved species to sulfate ion, and presence in the rain of background strong acid or base. Expressions were developed to predict the composition of raindrops as a function of fall distance, the time scale of atmospheric SO_2 removal, and ground level composition transients during a rain event. Illustrative calculations were made for single drop sizes and for the full spectrum of a model drop-size distribution, with the following results. In the absence of bisulfite oxidation and with an acidic background pH ($pH_o = 4$) the composition of rain was in equilibrium with SO_2 in the atmosphere after falling 100 to 200m through a mixed layer of pollutant. In contrast, the equilibrium composition was not reached within a fall distance of 2000m for a basic background pH ($pH_o = 10$). Furthermore, a unimodal distribution of pH with drop size was found in initially neutral or acidic rain whereas a bimodal distribution appeared with a strongly basic background pH. Introduction of bisulfite oxidation led to enhanced SO_2 uptake at $pH_o = 4$, and diminished uptake at $pH_o = 10$. Also, rejection of SO_2 from raindrops of small size was found in the presence of oxidation at $pH_o = 10$. Half-lives for SO_2 removal from the atmosphere at a 1 mm/hr rainfall rate and a mixed layer height of 1 Km ranged from hours to days depending on background-pH-and initial SO_2 atmospheric concentration.

The washout of sulfur dioxide from the atmosphere is a phenomenon which contributes to the production of so-called "acid rain" (Likens et al., 1972) and at the same time helps in the cleansing of the atmosphere. Effective models of the washout process are useful in predicting the composition of rain and the time scale for SO_2 removal. Two principal kinds of washout models have been devised in the past: physical models, exemplified by the work of Hales and his colleagues (Dana et al., 1973; Hales et al., 1973), and chemical models, stemming primarily from the work of Scott and Hobbs (1967). The physical models are mass transfer models in which the soluble gas is nominally regarded as inert but has a distribution coefficient which varies with SO_2 uptake, thereby taking into account in an approximate way the variation in hydrogen ion concentration which occurs as SO_2 dissolves in the falling rain drops. In the chemical models, mass transfer is taken to be infinitely rapid. Consequently the composition of the falling rain is always that in equilibrium with the concentration of SO_2 in the atmosphere, subject to the electroneutrality condition and to the extent of production of sulfate ion by oxidation of bisulfite and sulfite ion. In the present paper, the two models are combined by modifying the mass transfer relation for an inert gas to incorporate explicitly the ionic equilibria of the chemical model. The model which results allows for continuous variation of rain composition with fall distance. The model is used in illustrative fashion to calculate the composition of rain as a function of fall distance and to obtain the time scale for SO_2 removal from the atmosphere. A very simple chemical system is used as a basis for the model for the sake of ease of identification of the origin of effects predicted by the model. In a subsequent paper a chemical system more nearly approximating that of the atmosphere will be treated.

EQUILIBRIUM COMPOSITION OF RAIN

Knowledge of the equilibrium composition of rain is necessary in order to help in judging the efficacy of washout models since in the absence of oxidation such models should predict the equilibrium composition at large fall distances. In addition, a framework for the calculation of the equilibrium composition constitutes in itself an approximate model which may be compared with more refined representations, and these refined representations may or may not include liquid phase oxidation.

The expressions for the equilibrium composition of rain are derived below while keeping in mind a very simple picture, from a meteorological point of view, of the disposition of pollutant and cloud during a rain event. We consider a well-mixed layer of the atmosphere adjacent to the surface of the earth in which pollutant SO_2 is present at a concentration, $C_{SO_2,g}$. No SO_2 is found above this layer. Rain is formed above the layer and prior to entering the layer attains a background or initial concentration, C_{EX}, of a strong acid or strong base. C_{EX} is positive for a strong acid, negative for a strong base, and zero in the absence of both. If we denote the concentrations of hydrogen and hydroxyl ions in the rain above the mixed layer by $C_{H+}(0)$ and $C_{OH-}(0)$ then electroneutrality requires

$$C_{H+}(0) = C_{EX} + C_{OH-}(0) \tag{1}$$

We account for water ionization through the equilibrium expression,

$$K_w = C_{H+} C_{OH-} \tag{2}$$

From Equations (1) and (2), C_{EX} must be given by

$$C_{EX} = C_{H+}(0) - \frac{K_w}{C_{H+}(0)} \qquad (3)$$

In these equations we are assuming the anion of the strong acid or cation of the strong base to be univalent since the coefficient of C_{EX} in Equation (1) is unity.

From the above description, the chemical system treated involves simply dissolution of SO_2 in rain containing a strong acid or strong base. No other atmospheric gases or background solutes are present.

The composition of such rain in equilibrium with the atmosphere within the mixed layer may be derived from the following relations. The liquid phase equilibrium concentration of molecular SO_2 is given by Henry's law:

$$C_{SO_2} = \frac{C^*_{SO_2,g}}{H} \qquad (4)$$

The concentrations of bisulfite ion and hydrogen ion may be calculated as follows. Dissolved SO_2 and bisulfite ion participate in the equilibrium reaction

$$SO_2 + H_2O \rightleftharpoons H^+ + HSO_3^- \qquad (5)$$

with the position of equilibrium being determined by the relation

$$K_1 = \frac{C_{H^+} C_{HSO_3^-}}{C_{SO_2}} \qquad (6)$$

We assume the dissociation of HSO_3^- to $SO_3^=$ to be negligible.

Electroneutrality requires

$$C_{H^+} = C_{HSO_3^-} + C_{EX} + \frac{K_w}{C_{H^+}} \tag{7}$$

Upon substituting in Equation (6) for $C_{HSO_3^-}$ using Equation (7) and for C_{SO_2} using Equation (4), an equation for C_{H^+} is obtained whose solution is

$$C_{H^+} = 1/2\left[\sqrt{C_{EX}^2 + 4\left(K_1\, C_{SO_2,g}/H + K_w\right)} + C_{EX}\right] \tag{8}$$

Using Equation (8) in Equation (7):

$$C_{HSO_3^-} = 1/2\left[\sqrt{C_{EX}^2 + 4\left(K_1\, C_{SO_2,g}/H + K_w\right)} - C_{EX}\right] - \frac{K_w}{1/2\left[\sqrt{C_{EX}^2 + 4\left(K_1 C_{SO_2,g}/H + K_w\right)} + C_{EX}\right]} \tag{9}$$

The total concentration of sulfur compounds in the rain is

$$C_{S_T} = C_{SO_2} + C_{HSO_3^-} \tag{10}$$

The results of calculations using the above equations are shown in Figures 1 and 2. For these figures, $T = 298°K$, $H = 3.32 \times 10^{-2}$, and $K_1 = 1.3 \times 10^{-5}$ mole/cm^3 (Johnstone and Leppla, 1934). Also $K_w = 1.008 \times 10^{-20}$ mole^2/cm^6. C_{S_T} and C_{H^+} are plotted as a function of the concentration of SO_2 in air in the mixed layer with background pH as a parameter.

The two sets of curves in Figures 1 and 2 appear virtually identical except that the ordering of the background pH values is reversed between the two figures. They would, in fact, be identical if $C_{S_T} >> C_{SO_2}$ or, equivalently, if $C_{S_T} \approx C_{HSO_3^-}$, since as one can see from Equations (8) and (9), with K_w small,

$C_{HSO_3^-}(C_{EX}) \equiv C_{H^+}(-C_{EX})$. C_{SO_2} is in fact never greater than about two percent of C_{S_T}, thus explaining the near identity of the two figures.

The total sulfur content and hydrogen ion concentration of the rain are quite sensitive to background pH at low concentrations of SO_2 in air and become less so as this concentration increases. Thus, C_{S_T} and C_{H^+} vary over roughly two orders of magnitude as the background hydrogen ion concentration varies over six orders of magnitude at 10ppb SO_2 but over about one decade for the same variation at 100ppb. For the ranges of pH_0 and $C_{SO_2,g}$ shown in the figures, the maximum range of equilibrium pH is from 3.7 to 6.8, and of C_{S_T} is from 0.16 to 190 μ-mole/liter.

If the composition of all raindrops were in equilibrium with $C_{SO_2,g}$ by the time the drops arrived at the ground, then that composition would be given by Equations (4), (8) and (9) as shown in Figures 1 and 2.

WASHOUT MODEL

The extent to which the assumption of equilibrium is valid may be examined by constructing a model which accounts for the rate of entry of SO_2 into the raindrops and for which the equilibrium composition given above is approached at large fall distances. In constructing such a model one may provide for liquid phase oxidation of the dissolved sulfur compounds to, say, sulfate ion. When the latter feature is incorporated the equilibrium composition discussed above will not be approached. A washout model incorporating oxidation will now be developed. When the equilibrium assumption is to be tested, oxidation may be eliminated by setting the oxidation rate constant equal to zero.

The disposition of cloud above a well-mixed layer containing pollutant and the presence of background acid or base are the same as described previously. Raindrops falling through the mixed layer are assumed to be spherical and to fall vertically at their terminal velocities. Diffusion or mixing within the drops is taken to be rapid so that no concentration gradients develop there. With this assumption the present model will place an upper limit on the rate of SO_2 uptake. It will be necessary to treat the case of the stagnant drop before a lower limit can be established.

The equilibrium (5) is assumed to be instantaneously established throughout the drop, and Henry's law, Equation (4), determines the SO_2 gas-liquid distribution at the air-water interface. The production of sulfate ion is assumed to result from bisulfate oxidation. When sulfate ion is present, the electroneutrality condition becomes

$$C_{H^+} = C_{HSO_3^-} + 2C_{SO_4^=} + C_{EX} + \frac{K_w}{C_{H^+}} \tag{11}$$

and the total sulfur compound concentration in a drop is

$$C_{S_T} = C_{SO_2} + C_{HSO_3^-} + C_{SO_4^=} \tag{12}$$

Equilibria involving bisulfate ion and sulfuric acid are neglected.

The rate of accumulation of all compounds of sulfur in each falling drop is taken to be equal to the rate of mass transfer of SO_2 across a stagnant air film surrounding each drop:

$$u_z \frac{d\, C_{S_T}}{dz} = \frac{3k_g}{R}\left(C_{SO_2,g} - C^*_{SO_2,g}\right) \tag{13}$$

where 3/R is the area-to-volume ratio of the drop.

Finally, we assume sulfate ion is produced by a reaction which is first order with respect to bisulfite ion:

$$u_z \frac{d\, C_{SO_4^=}}{dz} = k_{ox}\, C_{HSO_3^-} \tag{14}$$

The two differential equations, Equations (13) and (14), with appropriate initial conditions, together with the algebraic relations, Equations (4), (6), (11) and (12), constitute the formulation of the problem. These equations can be reduced to two simultaneous differential equations in C_{H^+} and $C_{SO_4^=}$ as follows. From Equations (6) and (11) one can derive

$$C_{HSO_3^-} = C_{H^+} - 2C_{SO_4^=} - C_{EX} - \frac{K_w}{C_{H^+}} \tag{15}$$

$$C_{SO_2} = \frac{1}{K_1} C_{H^+}\left(C_{H^+} - 2C_{SO_4^=} - C_{EX} - \frac{K_w}{C_{H^+}}\right) \tag{16}$$

Equation (12) is differentiated with respect to z, and, in the resulting equation $C_{HSO_3^-}$ and C_{SO_2} are eliminated using Equations (15) and (16):

$$\frac{d\,C_{S_T}}{dz} = \frac{d}{dz}\;\frac{1}{K_1} C_{H^+}\left(C_{H^+} - 2C_{SO_4^=} - C_{EX} - \frac{K_w}{C_{H^+}}\right) + \frac{d}{dz}\left(C_{H^+} - 2C_{SO_4^=} - C_{EX} - \frac{K_w}{C_{H^+}}\right) + \frac{d}{dz} C_{SO_4^=} \tag{17}$$

Upon performing the indicated differentiations and collecting terms, one obtains

$$\frac{d\,C_{S_T}}{dz} = \frac{1}{K_1}\left[2C_{H^+} - 2C_{SO_4^=} - C_{EX} + K_1\left(1 + \frac{K_w}{C^2_{H^+}}\right)\right]\frac{d\,C_{H^+}}{dz} - \frac{1}{K_1}\left(2C_{H^+} + K_1\right)\frac{d\,C_{SO_4^=}}{dz} \tag{18}$$

Upon substituting Equations (4), (16), and (18) in Equation (13), one finds

$$\frac{1}{K_1}\left[2C_{H^+} - 2C_{SO_4^=} - C_{EX} + K_1\left(1 + \frac{K_w}{C^2_{H^+}}\right)\right]\frac{d\,C_{H^+}}{dz} - \frac{1}{K_1}\left(2C_{H^+} + K_1\right)\frac{d\,C_{SO_4^=}}{dz}$$
$$= \frac{3kg}{u_z R}\left[C_{SO_2,g} - \frac{H}{K_1} C_{H^+}\left(C_{H^+} - 2C_{SO_4^=} - C_{EX} - \frac{K_w}{C_{H^+}}\right)\right] \tag{19}$$

From Equations (14) and (15),

$$\frac{d\,C_{SO_4^=}}{dz} = \frac{k_{ox}}{u_z}\left(C_{H^+} - C_{EX} - 2C_{SO_4^=} - \frac{K_w}{C_{H^+}}\right) \tag{20}$$

Equations (19) and (20) are the washout model equations. They are to be solved subject to the initial conditions

$$z = 0,\; C_{H^+} = C_{H^+}(0) \tag{21}$$

$$C_{SO_4^=} = 0 \tag{22}$$

In the illustrative calculations that follow, Equations (19) and (20) were integrated numerically using the fourth order Runge-Kutta-Gill method. After obtaining C_{H^+} and $C_{SO_4^=}$ in this way, $C_{HSO_3^-}$ and then C_{SO_2} were found using Equations (7) and (6).

Test of Equilibrium Assumption. This assumption was tested by setting k_{ox} equal to zero in the integration of Equations (19) and (20). Calculations were made using values of u_z as given by Gunn and Kinzer (1949), and mass transfer coefficients obtained from the Frössling correlation (Frössling, 1938):

$$\frac{2k_g R}{D_{SO_2}} = 2.0 + 0.6\left(\frac{2Ru_z \rho_f}{\mu_f}\right)^{1/2}\left(\frac{\mu_f}{\rho_f D_{SO_2}}\right)^{1/3} \tag{23}$$

Values of μ_f/ρ_f and D_{SO_2} were the same as those used by Hales, et al. (1973). Calculations were made for $C_{SO_2,g}$ = 10ppb for drop radii of 0.1 and 1.0mm and for background pH values of 4 and 10. These values of R roughly represent extremes of this variable, and we assume the same is true for the chosen values of pH_o. The results of the calculations are plotted as the solid curves in Figures 3 to 6. Transients are shown for C_{H^+}, C_{SO_2}, and C_{S_T}, the latter being essentially equal to $C_{HSO_3^-}$ here as well as in the equilibrium calculations.

At a background pH of 4 there is relatively little capacity for sulfur compounds in the rain (Figure 1) and little change occurs in C_{H^+} as a result of dissolution of this equilibrium capacity (Figure 2). Accordingly at pH_0 = 4 (Figures 3 and 4) the washout model shows essentially no change in C_{H^+} as SO_2 dissolves in the drops. For the small drop (Figure 3) the C_{SO_2} transient approaches equilibrium closely within a few meters, whereas for the large drop a fall distance of about 400m is required. With essentially no change in C_{H^+} with fall distance, the C_{S_T} or $C_{HSO_3^-}$ transient is then a reflection of the C_{SO_2}

transient. From Gunn and Kinzer's data, u_z is 72 cm/sec for the small drop and 649 cm/sec for the large drop. From Equation (23), k_g is 26.9 cm/sec for the small drop and 14.0 cm/sec for the large drop. The values for the coefficient, $3k_g/u_zR$, in Equation (19), representing the combined effects of drop size on area-to-volume ratio, mass transfer coefficient, and fall velocity, are 112.1 and 0.647 cm^{-1} for the small and large drops, respectively. This difference of more than two orders of magnitude accounts for the difference in fall distances required for a close approach to equilibrium in the absence of oxidation.

At pH_o = 10 equilibrium is reached for the small drop (Figure 5) for all species at a fall distance of the order of 25m, but for the large drop (Figure 6) it is not approached at all within 2000m for hydrogen ion and SO_2, and at this distance C_{S_T} is about a half of its equilibrium value. The abrupt change in C_{H^+} and C_{SO_2} for the small drop at 25m occur because in effect at pH_o = 10 as the raindrops fall a strong base is being titrated by a weak acid and the end-point of the titration in the small drop is reached at a fall distance of 25m. At pH_o = 10 the capacity for HSO_3^- is very large, and neither C_{H^+} nor C_{SO_2} changes greatly from their initial values until $C_{HSO_3^-}$ is close to its equilibrium value. For the large drop it appears that $C_{HSO_3^-}$ would reach its equilibrium value at a fall distance of the order of 4000m or more whereupon C_{H^+} and C_{SO_2} would rise suddenly to their equilibrium values.

The rate at which SO_2 enters a drop of a given size and hence the fall distance at which the titration end-point is reached is determined by the value of the factor $3k_g/u_zR$ in Equation (19). It evidently happens that the ranges of raindrop sizes, terminal velocities, and mass transfer coefficients are such that titration end-points are predicted to occur for well-mixed small drops over fall distances which are less than physically significant mixed-layer heights. The consequence of this observation is that bimodal distributions of pH with drop size are predicted. Small drops would be acidic and large drops, basic. We will show typical variations of pH with R at a given fall distance later in the paper.

In summary, concerning the equilibrium assumption for well-mixed drops, it appears to be a good assumption for low initial pH for all reasonable drop sizes for fall distances of 500m or more. Also, the variation of pH with R would be small. For high initial pH, the assumption is good for small drops at small distances and very large distances are required for large drops. A bimodal pH distribution might be expected for high initial pH.

Influence of Oxidation. In the presence of oxidation Equations (19) and (20) were integrated with $k_{ox} = 1 \times 10^{-3}\ sec^{-1}$. This value of the oxidation rate constant corresponds to a bisulfite ion half-life of 11.6 min, comparable to the shortest half-lives commonly estimated (7).

The results of the integration for the same values of $C_{SO_2,g}$, pH_o, and R used in the previous section are represented by the dashed curves in Figures 3 to 6. The results for $pH_o = 4$ (Figures 3 and 4) and for the small drop at $pH_o = 10$ (Figure 5) are initially similar to those in the absence of oxidation in that a pseudo-equilibrium composition near the true equilibrium composition in the absence of oxidation is first approached. However, the relations in the presence of oxidation subsequently depart from their pseudo-equilibrium values as the oxidation of HSO_3^- progresses. The conversion of a bisulfite ion to a sulfate ion requires introduction of a hydrogen ion to maintain charge balance. The net effect of this requirement as the integration of the system of differential equations proceeds to greater fall distances is that C_{H^+} increases beyond its pseudo-equilibrium value. The pseudo-equilibrium value for $C_{HSO_3^-}$ is a maximum value and $C_{HSO_3^-}$ decreases at greater fall distances. The decrease comes about primarily in order to satisfy the equilibrium relation, Equation (6), responding to the increase in C_{H^+}. The changes in $C_{HSO_3^-}$ and C_{H^+} with z are greater at higher initial pH values. For the large drop at $pH_o = 10$ (Figure 6), pseudo-equilibrium is not attained within a fall distance of 2000m. The transients in C_{S_T}, C_{H^+}, and C_{SO_2} are indistinguishable from those found in the absence of oxidation.

An interesting feature of the problem of washout with oxidation has to do with the C_{S_T} and C_{SO_2} transients. At a low initial pH (Figures 3 and 4), C_{S_T} increases with fall distance beyond its pseudo-equilibrium value. The quantities, C_{H^+}, C_{SO_2}, and $C_{HSO_3^-}$ are relatively insensitive to the introduction of oxidation. Thus the increase in C_{S_T} following attainment of its pseudo-equilibrium value is closely equivalent to the production of sulfate ion. A markedly different situation is found at high initial pH (Figures 5 and 6). For the small drop, after attainment of its pseudo-equilibrium value, C_{S_T} actually decreases. For much of its subsequent fall the drop loses sulfur. Consistent with this behavior, C_{SO_2} rises above the value in equilibrium with $C_{SO_2,g}$, thus indicating transfer of SO_2 back into the atmosphere. The decrease in C_{S_T} occurs because of the significantly increased values of C_{H^+} and the consequent lowered values of $C_{HSO_3^-}$. Then, after a fall distance of approximately 1 Km, C_{S_T} starts to increase again as production of sulfate ion overcomes the loss of HSO_3^-. Also, at this fall distance C_{SO_2} falls below the value in equilibrium with $C_{SO_2,g}$, indicating entry of SO_2 into the drop again. Conceivably a similar type of behavior might be observed in the large drop at $pH_o = 10$ after C_{S_T} reaches its pseudo-equilibrium value.

In summary, in the presence of oxidation, a pseudo-equilibrium composition is first established after fall distances closely equal to those required to establish true equilibrium in the absence of oxidation. Departures from this composition occur at greater fall distances which involve increased acidity, decreased $C_{HSO_3^-}$ and the appearance of sulfate ion. C_{S_T} may increase, decrease or remain nearly constant with fall distance, depending upon initial pH.

Rain Composition for a Model Drop-Size Distribution. The calculations described previously are for single drop sizes. The composition of rain found in a collection device at ground level includes contributions from a full spectrum of drop sizes. Thus the mixed average composition at ground level is equal to the flux of the species of interest for a given drop size, summed over all drop sizes, and divided by the rainfall rate. Thus, for $\langle C_{S_T}(h)\rangle$, for instance,

$$\langle C_{S_T}(h)\rangle = \frac{1}{p}\int_0^\infty u_z(R)\, C_{S_T}(R,h)\, w\, f(R)\, dR \qquad (24)$$

For purposes of illustration in calculations to follow the drop-size distribution, f(R), given by Best (1950) was used. The Best distribution is given by

$$f(R) = \frac{n}{a}\left(\frac{2R}{a}\right)^{n-1} e^{-\left(\frac{2R}{a}\right)^{n}} \qquad (25)$$

where R is in millimeters and

$$a = \alpha p^{\beta} \qquad (26)$$

where p is in mm/hr.

Also,

$$n = 2.25$$

$$\alpha = 1.30$$

$$\beta = 0.232$$

The volume fraction rain, w, in the atmosphere required in the evaluation of Equation (24) is given by Best as

$$w = cp^{f} \qquad (27)$$

where $c = 67$

$f = 0.846$

The Best distribution, Equation (25), is shown in graphical form in Figure 7. The drop size corresponding to the maximum in the distribution is referred to as the predominant drop, of radius R_p. It may be shown that

$$R_p = \left(\frac{n-1}{n}\right)^{\frac{1}{n}} \frac{a}{2} \qquad (28)$$

The radius of the predominant drop at a rainfall rate of 1 mm/hr is 0.50 mm.

Equation (24) is evaluated by first finding C_{S_T} (R,h) from the solution of Equations (19) and (20) and then performing the integration indicated in Equation (24). This procedure was followed for a rainfall rate of 1 mm/hr and otherwise for the conditions for the earlier calculation for single drop sizes. The Best distribution was divided into ten intervals of drop-radius increment 0.15 mm, ranging from 0 to 1.5 mm, and the trapezoidal rule was used in the integration. The results, which are shown in Figures 8 and 9, are, as expected, intermediate to those for the large and small drops at the same values of initial pH (Figures 3 to 6). Equilibrium or pseudo-equilibrium is attained at $pH_o = 4$ at 100 to 200 meters for all sulfur species. Neither equilibrium nor pseudo-equilibrium is attained for $pH_o = 10$ within a fall distance of 2000m.

he irregular transients for hydrogen ion and SO_2 at $pH_o = 10$ result from end-point transitions occurring successively in drops of the first four or five sizes, starting with the smallest. Such transitions did not occur for the larger drops within the first 2000m. If the integration had been continuous over the full drop size range rather than a summation for discrete drop sizes, smooth transients for C_{H^+} and C_{SO_2} would have been obtained.

Data generated during the calculation of the mixed-average concentration transients include the variation of composition with drop size as a function of fall distance. Figure 10 shows the variation of pH with drop size at z = 1000m with no oxidation and with initial pH as a parameter. Unimodal pH distributions were found at pH_o = 4 and 7 while at pH_o = 10 a two-level distribution was found. The proportion of the drops which is acidic increases with fall distance. In Figure 10 for pH_o = 10, the pH is acidic for drops less than 0.51mm in radius. For the Best distribution, at 2 mm/hr rainfall rate, 44 percent of the rainfall is contained in drops with radii less than this value. A bimodal distribution of pH in rain has been observed by Esmen and Fergus (1975). Calculations in the present paper predict such a distribution and suggest a reason for its existence. Esmen and Fergus' observations were preliminary with insufficient detail to make comparisons with present theory.

At pH_o = 4 and 7 the C_{S_T} transients for the predominant drop for a 1 mm/hr rainfall rate and for $C_{SO_2,g}(0)$ values from 1 to 1000ppb agreed with the mixed average transient to within six percent for fall distances greater than 500m. The same was true for pH_o = 10 for values of $C_{SO_2,g}(0)$ above 10ppb, but at smaller initial concentrations of SO_2 in air (down to 1ppb) C_{S_T} for the predominant drop was greater than the mixed average by as much as roughly 100 percent. hese observations made it possible in the calculations described in the next section on cleansing of the atmosphere to save computer time by making calculations based on the predominant drop rather than the full spectrum. The results should closely represent those for the full spectrum except for $C_{SO_2,g}(0)$ of about 10ppb and less at $pH_o = 10$.

Cleansing of the Atmosphere.—The equations developed for predicting rain composition, Equations (19) and (20), can be used to estimate the time scale for SO_2 removal by the washout process and the magnitude of rain composition changes during a rain event. In applying these equations to this task, it is assumed as before that no concentration gradients develop in the mixed layer containing the pollutant and it is assumed that the time for rain to fall to the ground is short compared to the time to reduce the atmospheric concentration of SO_2 significantly. Before discussing the manner in which Equations (19) and (20) are used in characterizing atmospheric cleansing, this latter assumption will be checked for the Best distribution at, say, a rainfall rate of 1 mm/hr and a mixed layer height of 1 Km. For the smallest drop size interval considered in the integration of Equation (24), the mean drop radius is 0.075mm for which according to Gunn and Kinzer $u_z = 48$ cm/sec. For a 1 Km fall distance, the residence time for such a drop is about 35 min. For all larger drops, the residence time will be shorter. Thus if the calculations to follow predict washout times which are long compared to 35 min then the second assumption above will be valid and the calculation accepted.

When both assumptions are valid then one may state that the rate of loss of SO_2 from a box-shaped volume of air of height equal to the height of the mixed layer and of horizontal cross section A is equal to the rate of arrival at the ground in rain of all sulfur compounds:

$$-(1 - w)\ hA \frac{d\ C_{SO_2,g}}{dt} = pA\ \langle C_{S_T}(h)\rangle \quad (29)$$

where $\langle C_{S_T}(h)\rangle$ is obtained from Equation (24) as described previously. Upon integrating this equation from the onset of rainfall to time t after onset,

$$t = (1 - w)\ \frac{h}{p} \int_{C_{SO_2,g(t)}}^{C_{SO_2,g}(0)} \frac{d\ C_{SO_2,g}}{\langle C_{S_T}(h)\rangle} \quad (30)$$

Equation (30) is evaluated by first integrating Equations (19) and (20) over the fall distance h for desired values of rainfall rate and initial pH, and for a series of SO_2 concentrations in air, ranging between some desired initial and final values. In this integration of Equations (19) and (20) for, say, the Best distribution, calculations are made either for the full spectrum or for the predominant drop-size. The relation between $C_{SO_2,g}$ and $\langle C_{S_T}(h)\rangle$ thus developed is used in Equation (30) to relate these quantities to washout time. During the course of calculating $\langle C_{S_T}(h)\rangle$, the complete ground level rain composition history is generated.

The procedure outlined above was followed for the predominant drop for a rainfall rate of 1 mm/hr, for a fall distance of 1 Km and for initial concentrations of SO_2 in air ranging from 1 to 1000ppb, and for the k_{ox} and initial pH values used earlier. Sample results are shown in Figures 11 to 13.

In Figure 11, $t_{1/2}$, the time to remove 50 percent of the SO_2 present initially in the atmosphere, is shown as a function of initial SO_2 concentration and initial pH with HSO_3^- oxidation absent. The half-life is seen to be sensitive to both $C_{SO_2,g}(0)$ and pH_o. Almost all of the half-lives shown are of the order of

5 to 10 hr or longer, are thus long compared to residence times near the small drop-size end of the spectrum, and therefore satisfy the assumptions implicit in the calculation. The vertical portion of the curve for $pH_o = 10$ is the portion for which the predominant drop transient overestimates the mixed average transient by as much as a factor of two. The true SO_2 half-life in this region is thus as much as twice the value shown. The vertical portion of the curve for $pH_o = 10$ corresponds to conditions in which, for most or all of the half-life period, SO_2 entry into the predominant drop occurs at the maximum possible rate for the existing atmospheric SO_2 concentration for the entire 1 Km fall distance. Under these conditions the half-life becomes independent of $C_{SO_2,g}(0)$. The effect of the presence of oxidation (not represented in Figure 11) is to reduce $t_{1/2}$ on a percentage scale at $pH_o = 4$, since C_{S_T} is greater with oxidation than without, and to increase $t_{1/2}$, again on a percentage scale, at $pH_o = 10$, since C_{S_T} is less with oxidation.

Some information concerning the time scale of removal of SO_2 from air has been given by Beilke and Georgii (Georgii and Beilke, 1966; Beilke and Georgii, 1968). They performed laboratory experiments on the time scale of removal using water sprays with measured drop-size distributions and rainfall rates. They also varied solution composition by addition of a strong acid, base or oxidant. Certain features of their experiments make it difficult to compare present theory with the Beilke and Georgii data. The water was sprayed upward into an SO_2-air atmosphere within a 1-m^3 chamber and then fell into a collector at the bottom of the chamber. Thus the drop velocity varied with time in a manner difficult to determine. Also, the water was recirculated. The composition of the sprayed water thus changed with time in a way which is not known. Beilke and Georgii's results are nevertheless interesting in that they reported an exponential decrease in $C_{SO_2,g}$ with time with half-lives of 7.5 to 25 min for a 2 mm/hr rainfall rate using distilled water. The half-lives were shorter for the more basic solutions and for neutral water to which an oxidant had been added. Relatively short half-lives would be expected for a small chamber volume.

Figure 12 shows the $C_{SO_2,g}$ transients developed during SO_2 removal for $pH_o = 7$ with $k_{ox} = 0$. The strong effect of the initial concentration of SO_2 in air is seen. At small $C_{SO_2,g}(0)$ the decay is essentially exponential while at larger $C_{SO_2,g}$ values a different dependence is found.

Figure 13 shows the concentration transients at ground level which occur during a rain event. For the conditions shown in the figure the SO_2 gas phase concentration decreases by about 62 percent in a 24-hr period, the pH increases by about 0.2 pH unit and the total sulfur concentration decreases by about 38 percent.

CONCLUDING REMARKS

The washout model described in the present paper was developed and applied for sulfur dioxide. It can be used for other reactive gases as well with appropriate modification. As Hales, et al. (1973) have done with their model, it may be applied to plumes from industrial stacks by assuming $C_{SO_2,g}$ in Equation (19) to vary suitably with position. Desirable extensions of the theory include treatment of the stagnant drop, inclusion of washout of other reactive gases, such as carbon dioxide and ammonia, and washout of acidic or basic particles.

NOTATION

a	constant in Best drop-size distribution, Equation (25)
c	constant in Best expression for water content in air during a rain event; see Equation (27)
C	concentration, $mole/cm^3$
D	diffusivity in air, cm^2/sec
f	constant in Best expression for water content in air during a rain event; see Equation (27)
f(R)	Best drop-size distribution function; fraction of liquid water in drops with radii between R and R + dR, mm^{-1}
h	height of mixed layer containing pollutant SO_2, cm
H	Henry's law constant for molecular SO_2, dimensionless
k_g	gas phase mass transfer coefficient, cm/sec
k_{ox}	rate constant for bisulfate oxidation, sec^{-1}
K_w	constant for water ionization, $mole^2/cm^6$
K_1	ionization constant for equilibrium (5) $mole/cm^3$
n	constant in Best drop-size distribution, Equation (25)
p	rainfall rate, mm/hr in Equations (26) and (27); otherwise, cm/sec
R	drop radius, mm in Equation (25); cm otherwise
R_p	predominant drop radius in Equation (28), mm
t	time, sec
u_z	drop terminal velocity, cm/sec
w	volume fraction rain in atmosphere, mm^3/m^3 in Equation (27); dimensionless otherwise.
y	$C_{H^+}/C_{H^+}(\infty)$, dimensionless
z	fall distance, cm

α	constant in Equation (26)
β	constant in Equation (26)
μ	viscosity, gm/cm-sec
ρ	density, gm/cm^3

Subscripts

EX	refers to background excess acid or base in raindrops
f	evaluated within gas film
i	refers to species i in liquid phase
i,g	refers to species i in gas phase
S_T	refers to total sulfur content
o	refers to initial condition

Superscript

*	refers to equilibrium condition

LITERATURE CITED

Beilke, S., and Georgii, H.-W. (1968) Investigation on the incorporation of sulfur-dioxide into fog- and rain-droplets. Tellus 20, 435-441.

Best, A. C. (1950) The size distribution of raindrops. Quart. J. Roy. Met. Soc. 76, 16-36.

Brimblecombe, P., and Spedding, D. J. (1974) The catalytic oxidation of micromolar aqueous sulfur dioxide. Atmospheric Environment 8, 937-945.

Dana, M. T., Hales, J. M., Slinn, W. G. N., and Wolf, M. A. (1973) Natural precipitation washout of sulfur compounds from plumes. U.S. Environmental Protection Agency Report EPA-R3-73-047, 204 p.

Esmen, N. A., and Fergus, R. B. (1975) SO_2-NH_3-particulate matter-H_2O system as related to the rainfall acidity. Presented in First International Symposium on Acid Precipitation and the Forest Ecosystem, Columbus, Ohio, May 12-15.

Frössling, N. (1938) The evaporation of falling drops. Gerlands Beitr. Geophys. 52, 170-216.

Georgii, H.-W., and Beilke, S. (1966) Atmospheric aerosol- and trace-gas washout. Final scientific report. Contract AF 61 (052) - 815, 55 p.

Gunn, R., and Kinzer, G. D. (1949) The terminal velocity of fall for water droplets in air. J. Meteorol. 6, 243-248.

Hales, J. M., Wolf, M. A., and Dana, M. T. (1973) A linear model for predicting the washout of pollutant gases from industrial plumes. A.I.Ch.E. Journal 19, 292-297.

Johnstone, H. F., and Leppla, P. W. (1934) The solubility of sulfur dioxide at low partial pressures. The ionization constant and heat of ionization of sulfurous acid. J. Am. Chem. Soc. 56, 2233-2238.

Likens, G. E., Bormann, F. H., and Johnson, N. M. (1972) Acid rain. Environment 14, 33-39.

Scott, W. D., and Hobbs, P. V. (1967) The formation of sulfate in water droplets. J. Atmos. Sci. 24, 54-57.

FIGURE CAPTIONS

Figure No.	Caption
1.	Total sulfur compound concentration at equilibrium ($k_{ox} = 0$). $T = 298°K$.
2.	Equilibrium hydrogen ion concentration ($k_{ox} = 0$). $T = 298°K$.
3.	Concentration transients in the small drop ($R = 0.1$ mm) at $pH_0 = 4$. $C_{SO_2,g} = 10$ ppb. $T = 298°K$.
4.	Concentration transients in the large drop ($R = 1.0$ mm) at $pH_0 = 4$. $C_{SO_2,g} = 10$ ppb. $T = 298°K$.
5.	Concentration transients in the small drop ($R = 0.1$ mm) at $pH_0 = 10$. $C_{SO_2,g} = 10$ ppb. $T = 298°K$.
6.	Concentration transients in the large drop ($R = 1.0$ mm) at $pH_0 = 10$. $C_{SO_2,g} = 10$ ppb. $T = 298°K$.
7.	The Best drop-size distribution (Best, 1950).
8.	Mixed average concentration transients at a rainfall rate of 1 mm/hr for the Best drop-size distribution. $C_{SO_2,g} = 10$ ppb, $pH_0 = 4$, $T = 298°K$.
9.	Mixed average concentration transients at a rainfall rate of 1 mm/hr for the Best drop-size distribution. $C_{SO_2,g} = 10$ ppb, $pH_0 = 10$, $T = 298°K$.
10.	Variation of pH with drop radius. $C_{SO_2,g} = 10$ppb, $h = 1000$m, $k_{ox} = 0$, $T = 298^oK$.
11.	Half-life for the sulfur dioxide washout process for a mixed layer height of 1 Km and a rainfall rate of 1 mm/hr. Based on calculations for the predominant drop ($R_p = 0.50$ mm) of the Best spectrum. $T = 298°K$. $k_{ox} = 0$.

Figure No.	Caption
12.	Sulfur dioxide gas phase transients during washout for a mixed layer height of 1 Km, and a rainfall rate of 1 mm/hr. Based on calculations for the predominant drop (R_p = 0.50 mm) of the Best spectrum for a rainfall rate of 1 mm/hr. $pH_0 = 7$, $k_{ox} = 0$, T = 298°K.
13.	Concentration transients during rainfall at a rate of 1 mm/hr. Based on calculations for the predominant drop (R_p = 0.50 mm) of the Best spectrum for a rainfall rate of 1 mm/hr. h = 1 Km, $pH_0 = 7$, $k_{ox} = 1 \times 10^{-3}\ sec^{-1}$, T = 298°K.

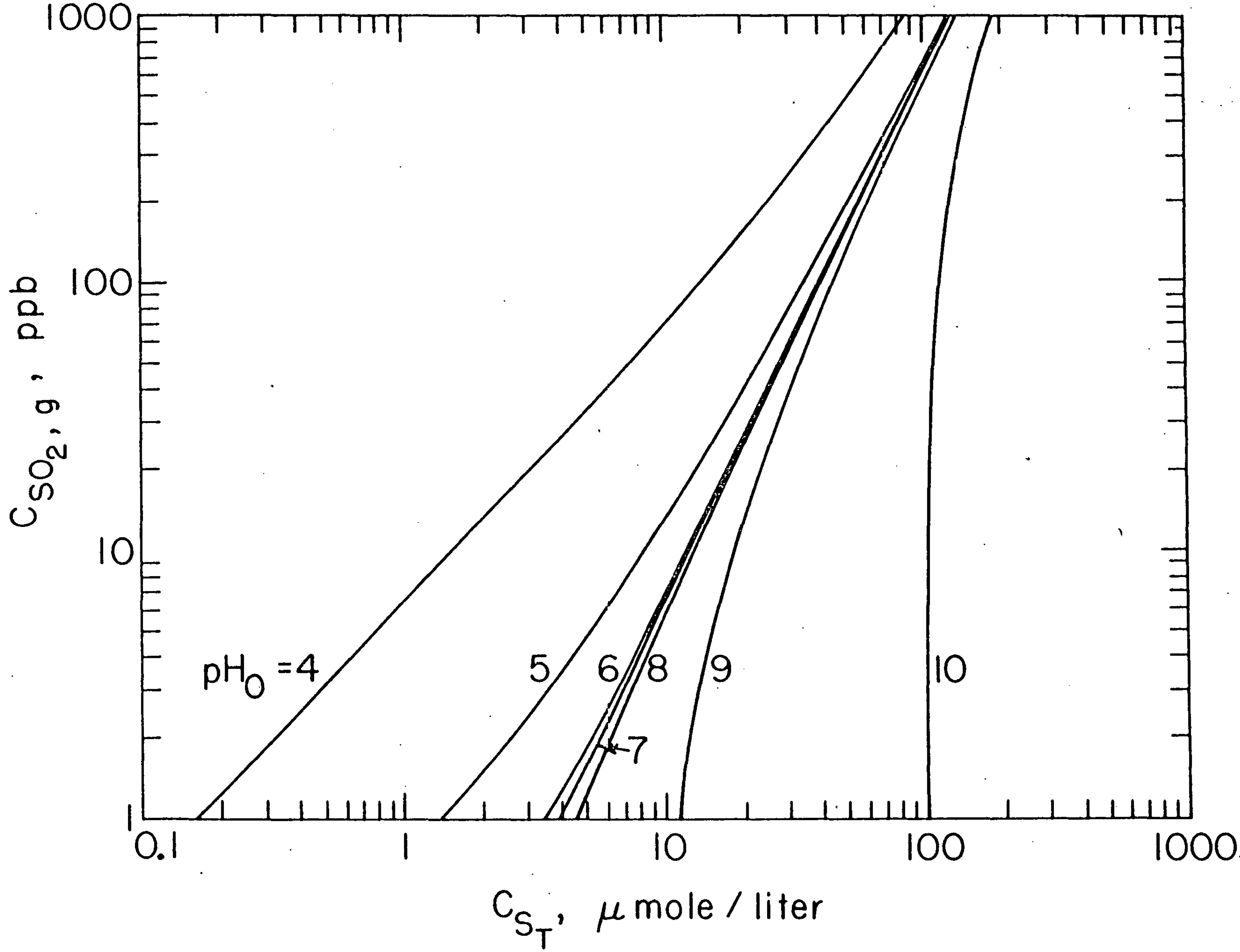
1000
100
10
1
$C_{SO_2,g}$, ppb
0.1
1
10
100
1000
C_{S_T}, μ mole / liter
pH_0 =4
5
6
8
9
10
7

Figure 1

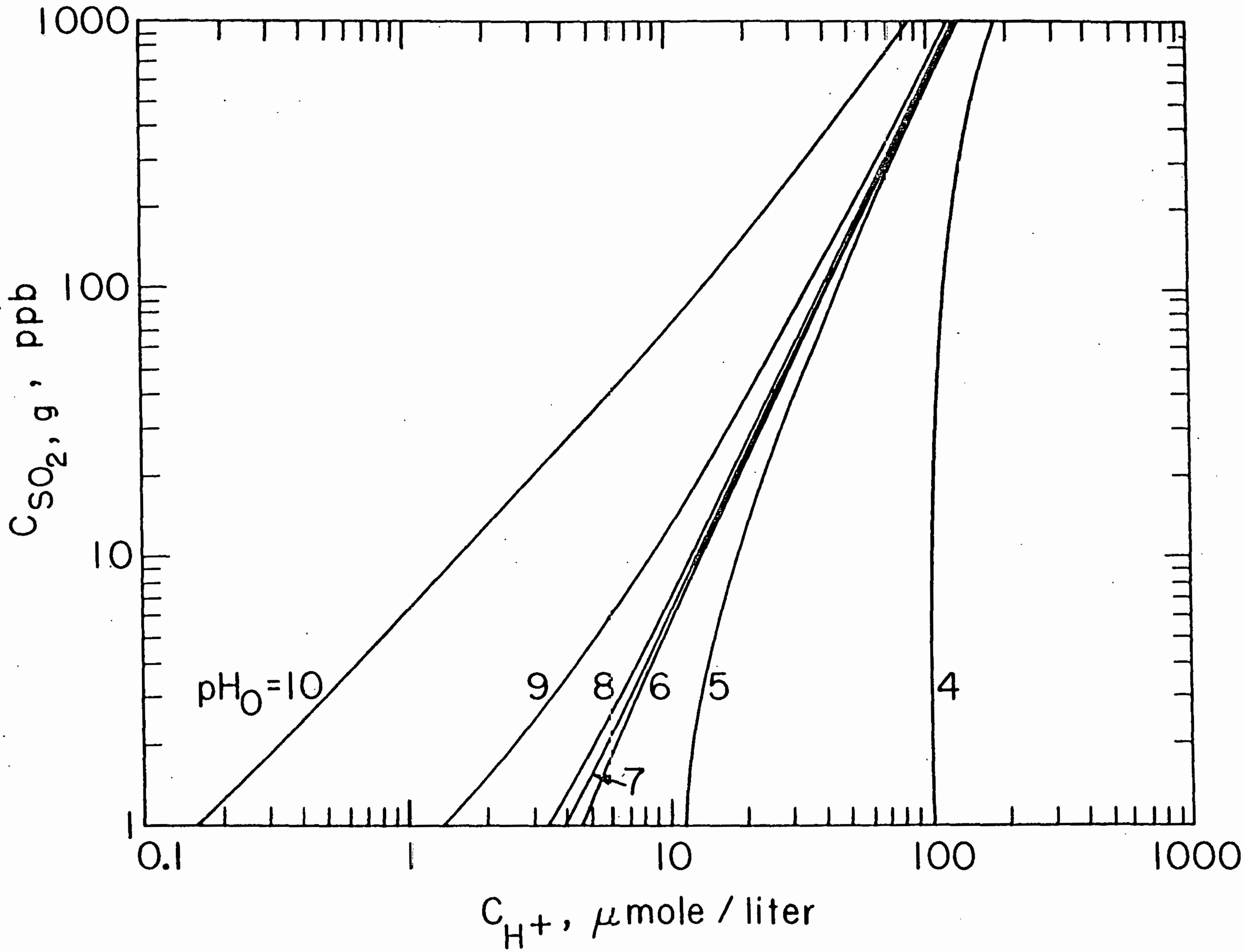

1000
100
10
1
0.1
1
10
100
1000
$C_{SO_2,g}$, ppb
C_{H^+}, μmole / liter
pH$_0$=10
9
8
6
5
4
7

Figure 2

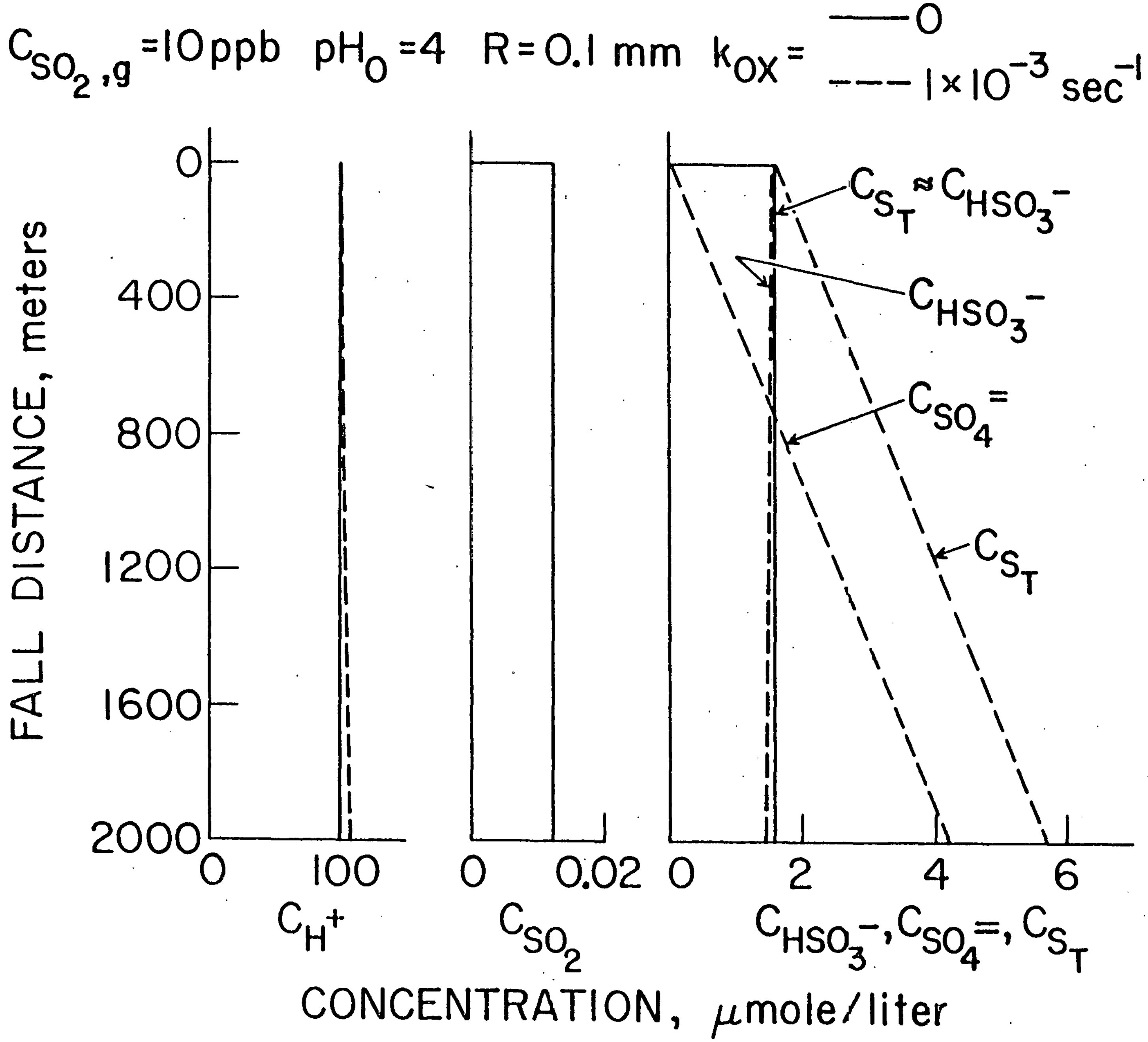
$C_{SO_2,g}$ = 10 ppb pH$_0$ = 4 R = 0.1 mm k_{OX} = —— 0 / - - - 1×10^{-3} sec^{-1}
FALL DISTANCE, meters
0
400
800
1200
1600
2000
0
100
C_{H^+}
0
0.02
C_{SO_2}
0
2
4
6
$C_{S_T} \approx C_{HSO_3^-}$
$C_{HSO_3^-}$
$C_{SO_4^=}$
C_{S_T}
$C_{HSO_3^-}, C_{SO_4^=}, C_{S_T}$
CONCENTRATION, μmole/liter

Figure 3

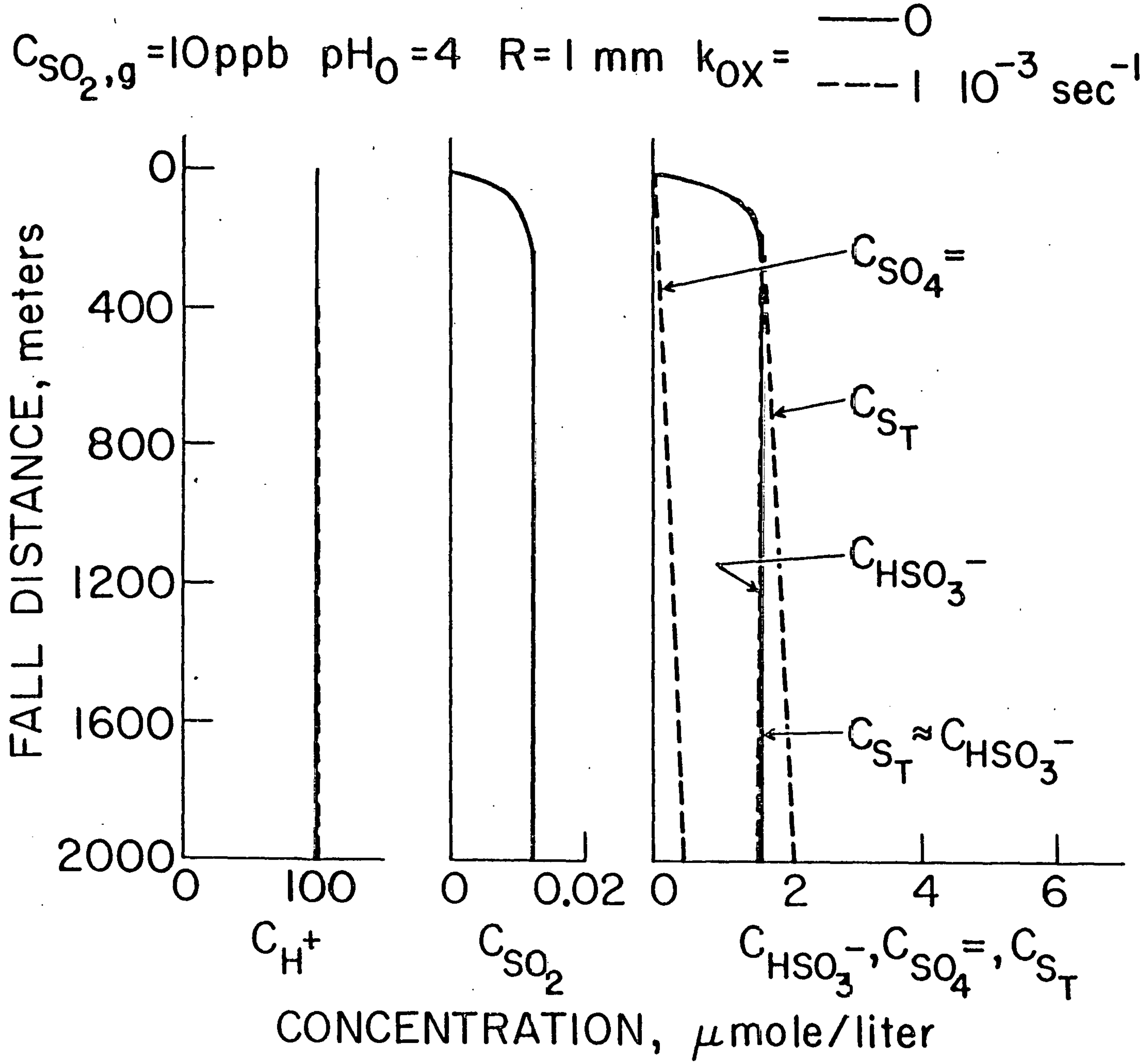

$C_{SO_2,g}$ = 10 ppb pH_0 = 4 R = 1 mm k_{OX} = —— 0 / --- 1 10^{-3} sec^{-1}
FALL DISTANCE, meters
0
400
800
1200
1600
2000
0
100
C_{H^+}
0
0.02
C_{SO_2}
0
2
4
6
$C_{HSO_3^-}$, $C_{SO_4^=}$, C_{S_T}
$C_{SO_4^=}$
C_{S_T}
$C_{HSO_3^-}$
$C_{S_T} \approx C_{HSO_3^-}$
CONCENTRATION, μmole/liter

Figure 4

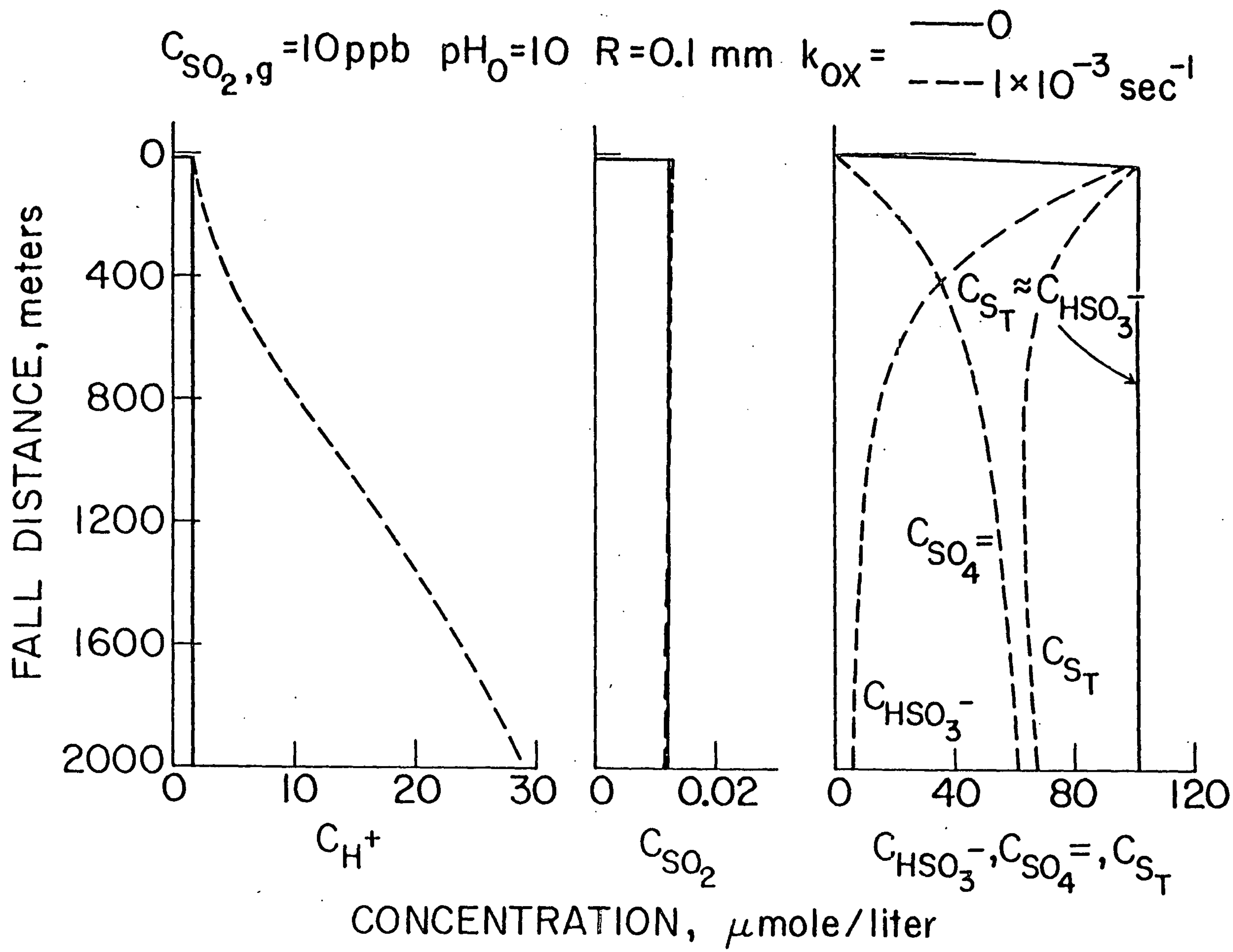
$C_{SO_2,g}$ =10 ppb pH$_0$=10 R=0.1 mm k_{OX} = —— 0 ---- 1×10^{-3} sec^{-1}
FALL DISTANCE, meters
0
400
800
1200
1600
2000
0
10
20
30
C_{H^+}
0
0.02
C_{SO_2}
0
40
80
120
$C_{HSO_3^-}$, $C_{SO_4^=}$, C_{S_T}
$C_{S_T} \approx C_{HSO_3^-}$
$C_{SO_4^=}$
C_{S_T}
$C_{HSO_3^-}$
CONCENTRATION, μmole/liter

Figure 5

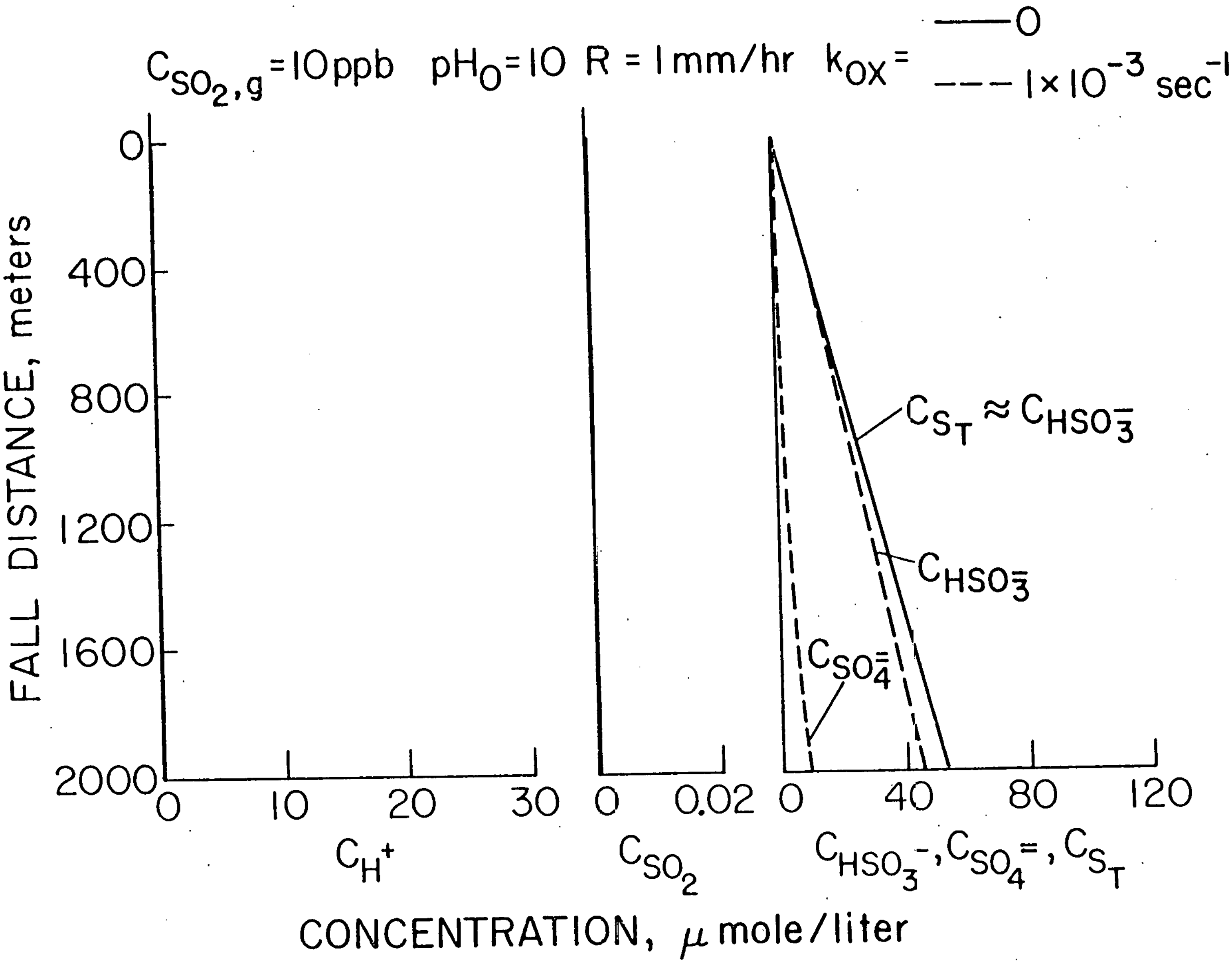

$C_{SO_2,g}$ = 10 ppb pH_0 = 10 R = 1 mm/hr k_{OX} =
—— 0
- - - 1×10^{-3} sec^{-1}
FALL DISTANCE, meters
0
400
800
1200
1600
2000
0
10
20
30
0
0.02
0
40
80
120
$C_{S_T} \approx C_{HSO_3^-}$
$C_{HSO_3^-}$
$C_{SO_4^=}$
C_{H^+}
C_{SO_2}
$C_{HSO_3^-}$, $C_{SO_4^=}$, C_{S_T}
CONCENTRATION, μ mole/liter

Figure 6

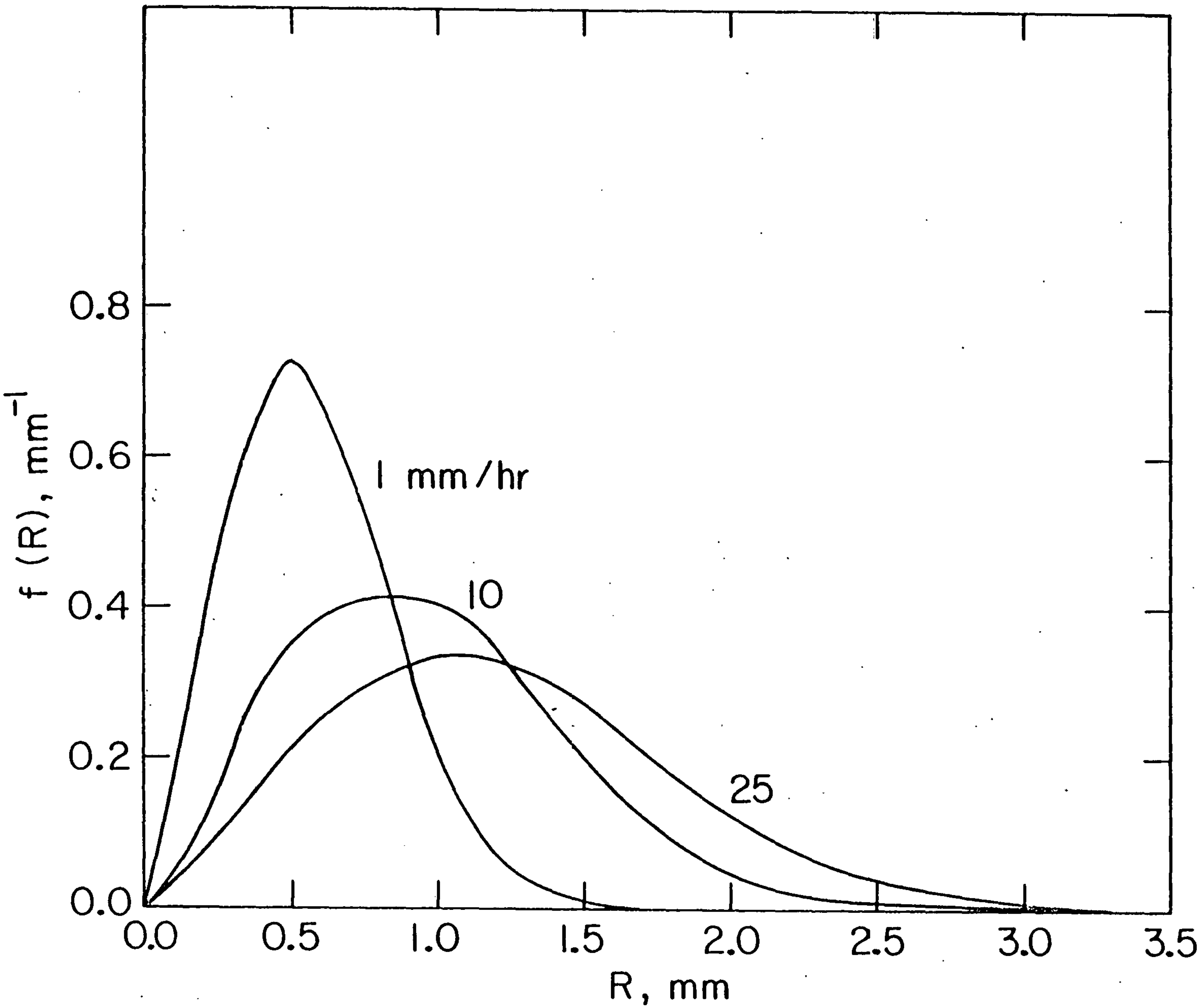

Figure 7

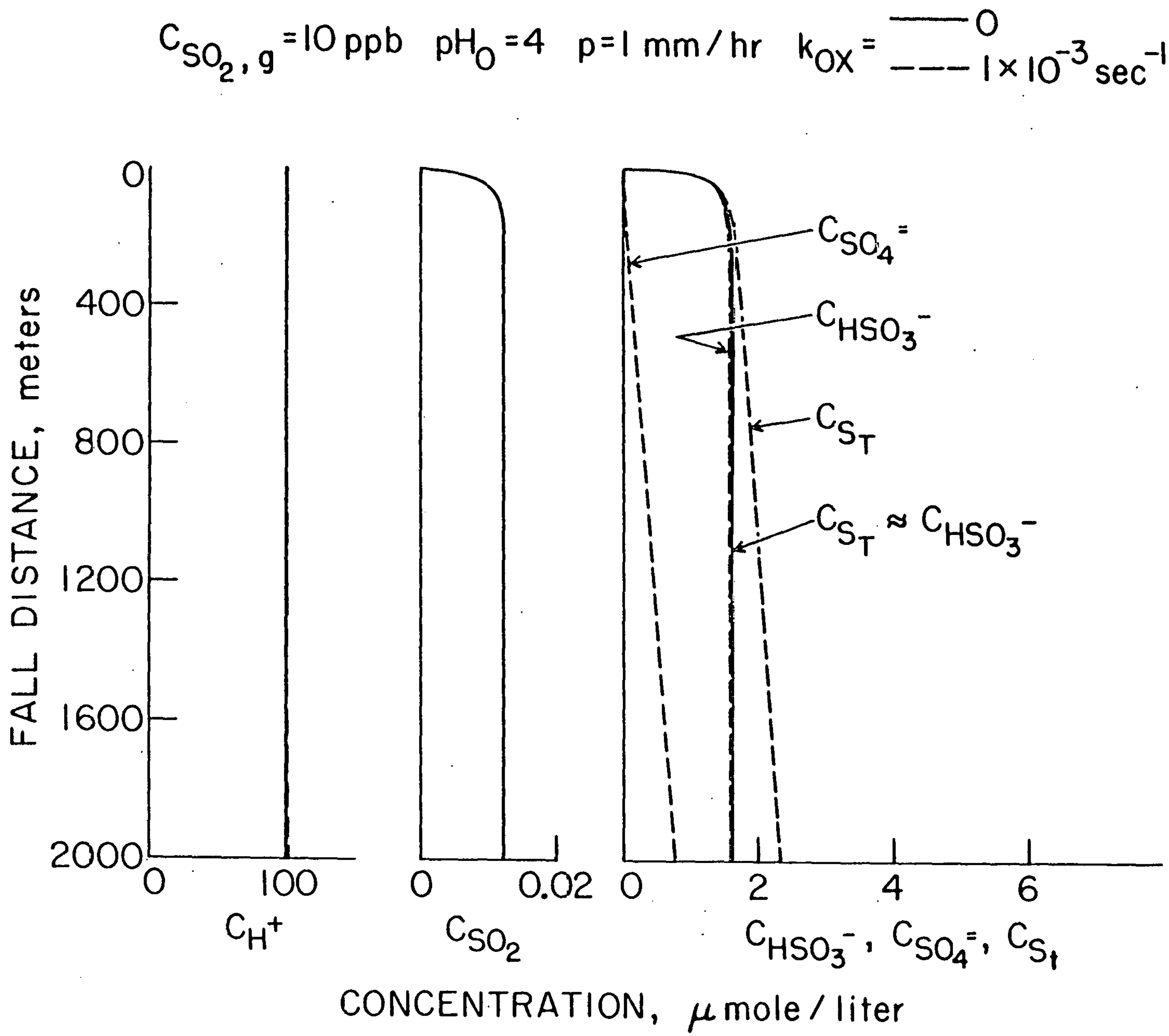
$C_{SO_2,g}$ = 10 ppb pH_0 = 4   p = 1 mm/hr k_{OX} = —— 0, - - - 1×10^{-3} sec^{-1}
FALL DISTANCE, meters
0
400
800
1200
1600
2000
0
100
C_{H^+}
0
0.02
C_{SO_2}
0
2
4
6
$C_{HSO_3^-}$, $C_{SO_4^=}$, C_{S_t}
$C_{SO_4^=}$
$C_{HSO_3^-}$
C_{S_T}
$C_{S_T} \approx C_{HSO_3^-}$
CONCENTRATION, μmole/liter

Figure 8

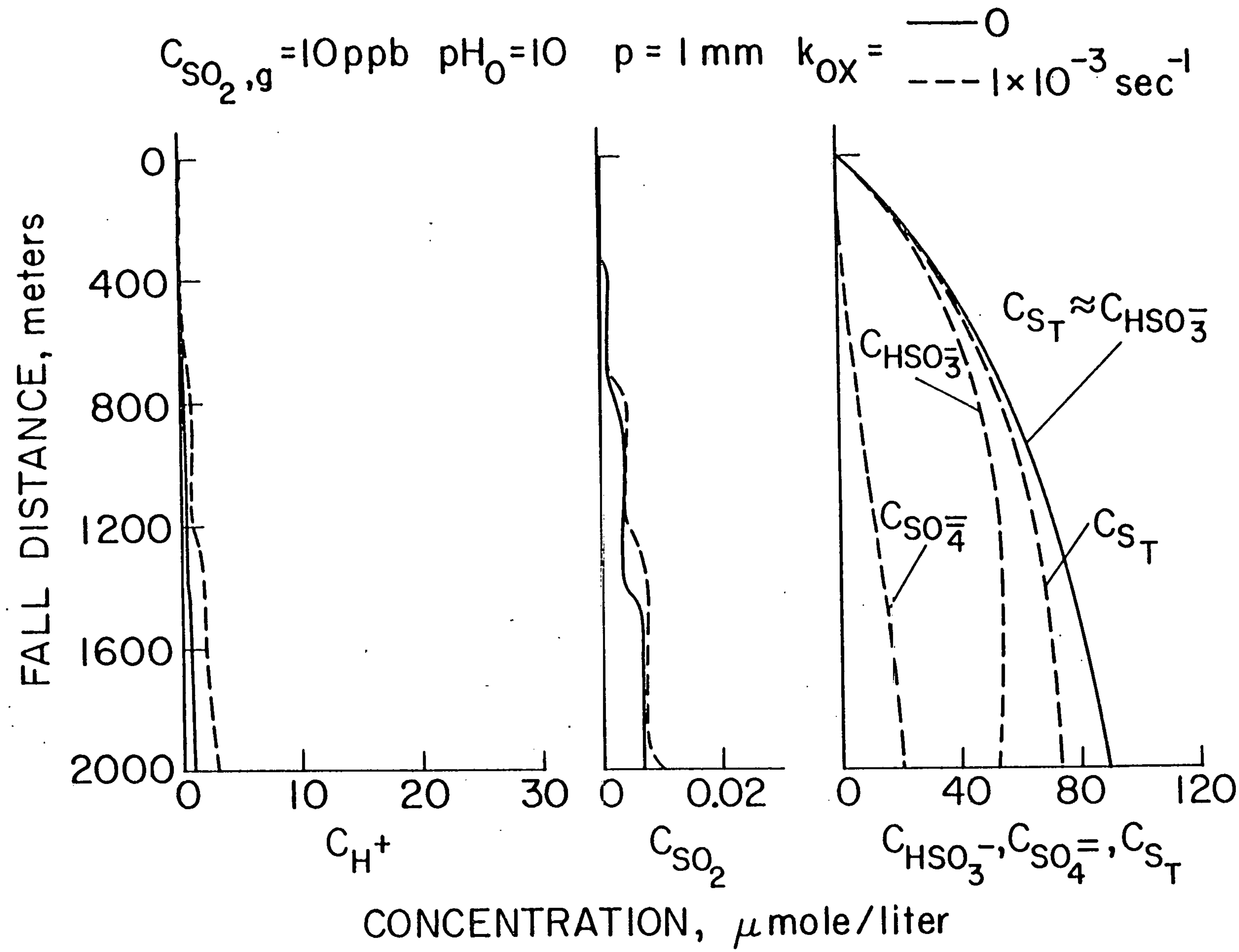
$C_{SO_2,g}$ = 10 ppb pH_0 = 10   p = 1 mm k_{ox} = —— 0, - - - 1×10^{-3} sec^{-1}
FALL DISTANCE, meters
0
400
800
1200
1600
2000
0
10
20
30
C_{H^+}
0
0.02
C_{SO_2}
0
40
80
120
$C_{S_T} \approx C_{HSO_3^-}$
$C_{HSO_3^-}$
$C_{SO_4^=}$
C_{S_T}
$C_{HSO_3^-}, C_{SO_4^=}, C_{S_T}$
CONCENTRATION, μmole/liter

Figure 9

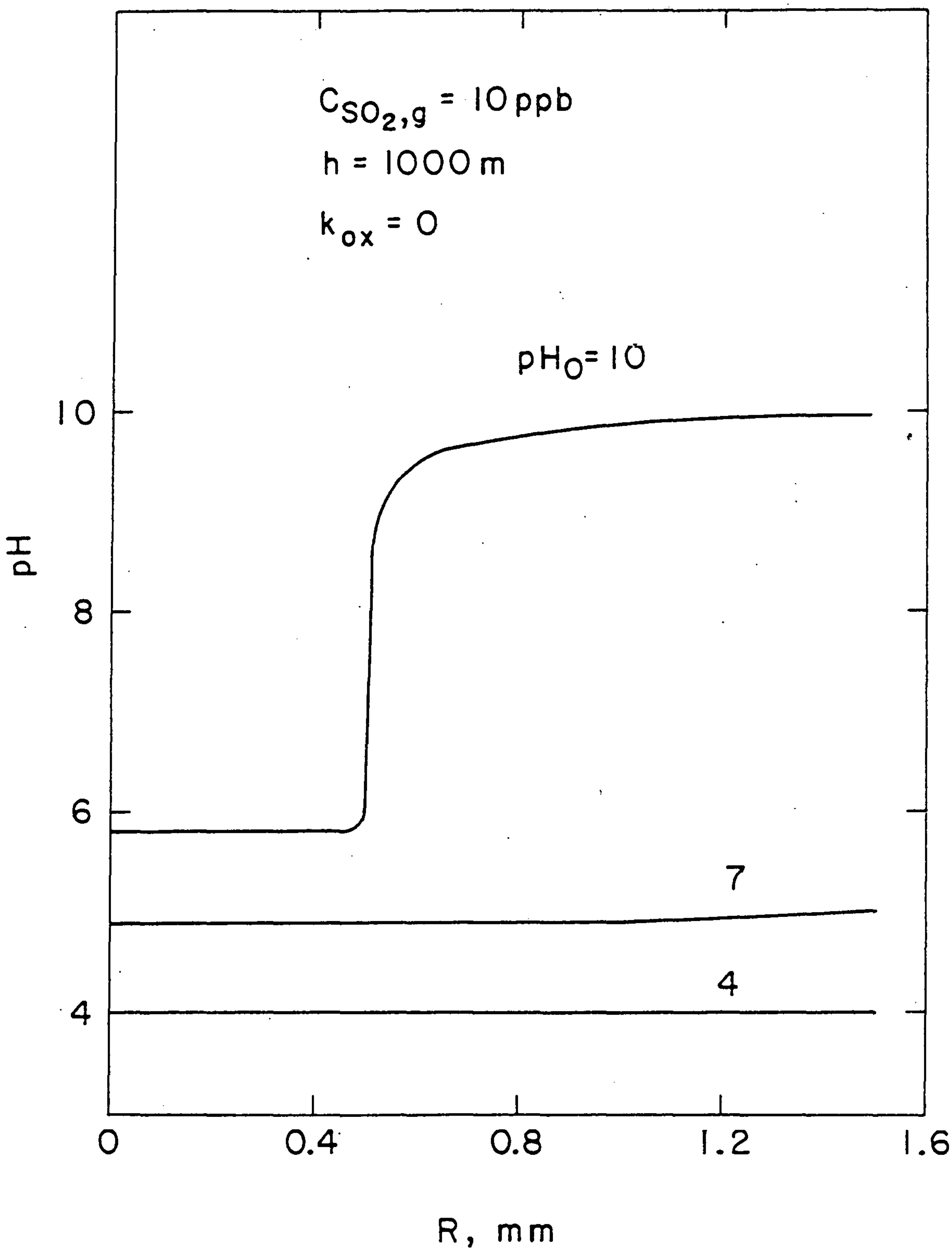

Figure 10

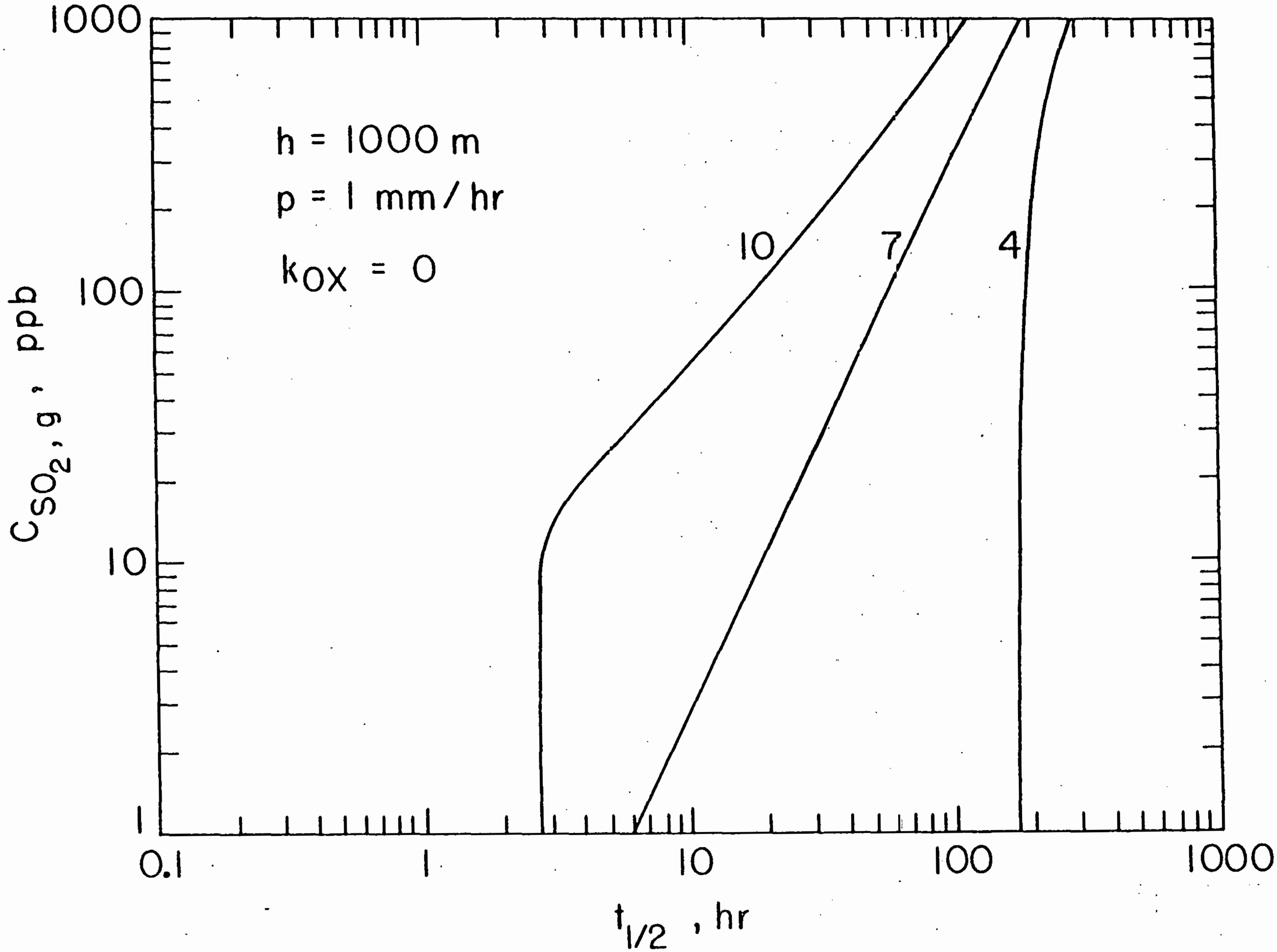

h = 1000 m
p = 1 mm/hr
k_{OX} = 0
10
7
4
$C_{SO_2,g}$, ppb
1000
100
10
1
0.1
1
10
100
1000
$t_{1/2}$, hr

Figure 11

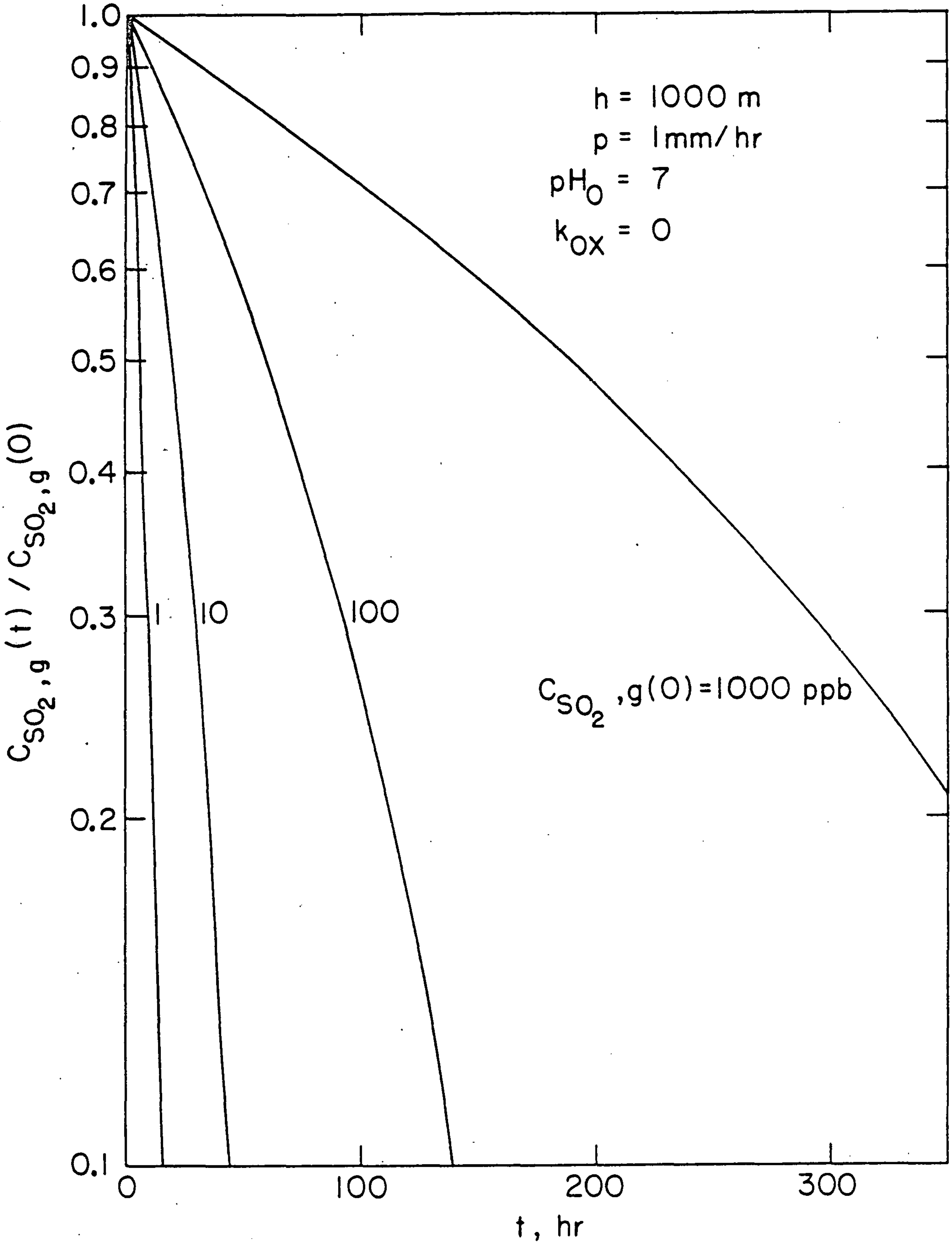
1.0
0.9
0.8
0.7
0.6
0.5
0.4
0.3
0.2
0.1
$C_{SO_2,g}(t) / C_{SO_2,g}(0)$
0
100
200
300
t, hr
h = 1000 m
p = 1mm/hr
pH_0 = 7
k_{OX} = 0
1
10
100
C_{SO_2},g(0)=1000 ppb

Figure 12

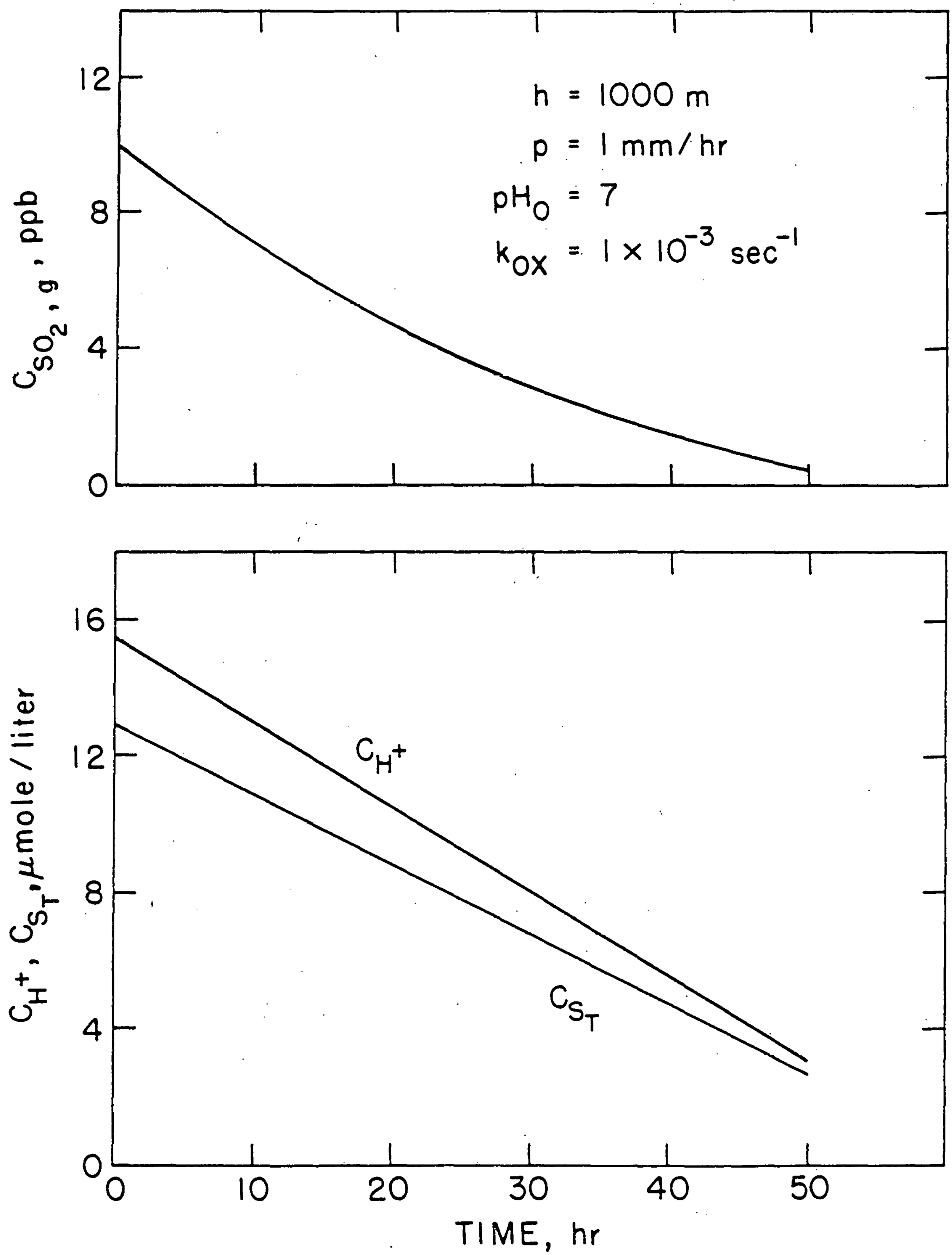

h = 1000 m
p = 1 mm/hr
pH_0 = 7
$k_{OX} = 1 \times 10^{-3}\ sec^{-1}$
$C_{SO_2,g}$, ppb
0
4
8
12
C_{H^+}
C_{S_T}
C_{H^+}, C_{S_T}, μmole / liter
0
4
8
12
16
0
10
20
30
40
50
TIME, hr

Figure 13